Restoration of Auditory Nerve Synapses in Cats by Cochlear Implants

D. K. Ryugo,[1,2]*† E. A. Kretzmer,[2]* J. K. Niparko[1]

Congenital deafness results in abnormal synaptic structure in endings of the auditory nerve. If these abnormalities persist after restoration of auditory nerve activity by a cochlear implant, the processing of time-varying signals such as speech would likely be impaired. We stimulated congenitally deaf cats for 3 months with a six-channel cochlear implant. The device used human speech-processing programs, and cats responded to environmental sounds. Auditory nerve fibers exhibited a recovery of normal synaptic structure in these cats. This rescue of synapses is attributed to a return of spike activity in the auditory nerve and may help explain cochlear implant benefits in childhood deafness.

In deaf humans, cochlear implants have restored hearing for many but not all recipients. The clinical consensus is that oral language development before deafness leads to the best outcomes. Among congenitally deaf children, the younger the age of implant activation, the better the aural language results (1). These clinical experiences imply that uncorrected congenital deafness introduces irreversible abnormalities in the developing central nervous system. In mammalian models of congenital deafness, the synaptic structure of auditory nerve endings is abnormal (2–4). Could the status of auditory nerve synapses represent an important link to the success or failure of cochlear implants?

One defect in the auditory nerve of congenitally deaf animals occurs at a large axosomatic ending of myelinated auditory nerve fibers called the endbulb of Held (2–4). Endbulbs have a calyxlike appearance that is formed from the main axon as several gnarled branches that arborize repeatedly to enclose the postsynaptic cell in a nest of en passant swellings and terminal boutons (5). They transmit signals from the auditory nerve fiber to the postsynaptic cell with a high degree of fidelity (6, 7) and are implicated in the pathways that process the temporal features of sound (8, 9). Congenitally deaf animals exhibit endbulbs with marked reduction in their branching (3, 10). Moreover, they contain fewer synaptic vesicles, and postsynaptic densities are longer and straighter (2, 3). These structural abnormalities have been associated with transmission irregularities at the synapse of endbulbs (11, 12) that may underlie loss of temporal res-

olution of midbrain (13) and cortical (14) neurons in neonatally deafened cats.

Electrical stimulation in deaf cats has resulted in improvements in temporal processing at the level of the auditory cortex (15) and inferior colliculus (16). Our goal was to test whether such benefits might be mediated through "rescue" of endbulb synapses. We sought to determine what happened to these synapses when spike activity was reintroduced to the auditory nerve. The synaptic status in implanted deaf animals may yield insights into the beneficial intervention effects reported for children who undergo implantation at a young age (17–19).

We compared auditory nerve endings in the cochlear nucleus of congenitally deaf cats fitted with a cochlear implant (n = 3) with those of normal-hearing cats (n = 3) and congenitally deaf cats (n = 4). Complete deafness of the

auditory nerve for the congenitally deaf cats was verified by the absence of acoustically evoked brainstem responses. Congenitally deaf cats were implanted at 2.5, 3, and 5 months of age. Following a 2- to 3-week recovery, implant hardware was programmed and the cats received stimulation for nearly 8 hours per day, 5 days per week. Electrically evoked compound action potentials (ECAPs) (Fig. 1) and behavioral responses were monitored monthly to verify continued function of each electrode and to ensure that signals were being delivered to the nerve (20). We were confident that environmental sounds had biological importance to the animals, because we could routinely "call" implanted cats for a food reward. After 3 months of stimulation, cats were euthanized by overdose of sodium pentobarbital and transcardially perfused with buffered fixative, and brain tissue was harvested for light and electron microscopic analysis. Tissue sections of the cochlear nucleus were histologically prepared using standard procedures for examination with an electron microscope (2).

In the anteroventral cochlear nucleus, auditory nerve synapses have a readily identifiable ultrastructural appearance (21, 22). Endbulbs contain clear, round synaptic vesicles (50 nm in diameter) and exhibit multiple asymmetric membrane thickenings with the somata of spherical bushy cells in the cochlear nucleus (Fig. 2). These membrane thickenings are called postsynaptic densities, contain transmitter receptors, and are assumed to represent the synaptic release sites. They are punctate, marked by dense material in the cytoplasm, and arched outward into the presynaptic endbulb. When individual synapses were followed through serial sections and reconstructed using computer software, their discrete nature was revealed by observing the surface of the postsynaptic
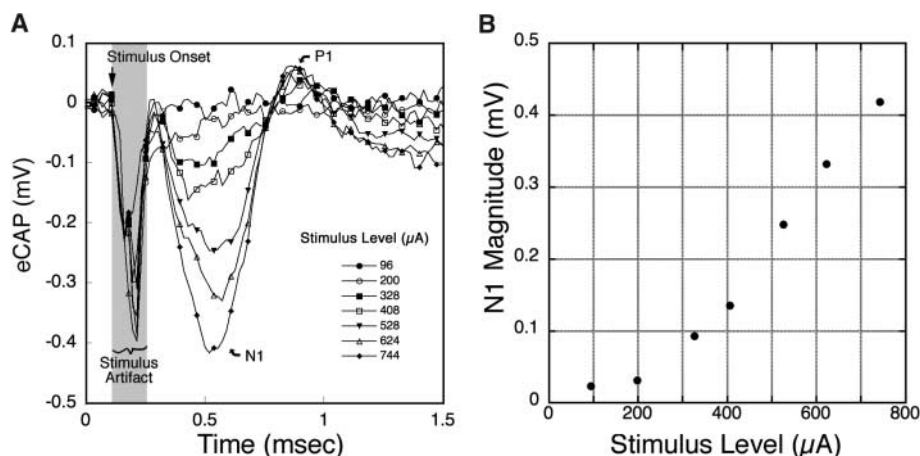

Fig. 1. (A) Recording of ECAP where stimulation was delivered by electrode 1 and recordings were collected from electrode 3. Electrode 1 is the most apical electrode. Stimulus onset and stimulus artifact are indicated, as are N1 and P1 potentials. This ECAP was representative of our cats and exhibited waveforms and peak latencies similar to what has been shown for humans (20). (B) N1-P1 amplitude as a function of stimulus level. Note the growth in response with increasing stimulus levels. These data suggest that electrical signals from the cochlear implant are entering the brain via the auditory nerve.

[1]Department of Otolaryngology-Head and Neck Surgery and [2]Department of Neuroscience, Johns Hopkins University Center for Hearing and Balance, 720 Rutland Avenue, Baltimore, MD 21205, USA.

*These authors contributed equally to this work.
†To whom correspondence should be addressed: dryugo@bme.jhu.edu

Fig. 2. Electron micrographs of endbulb (EB) synapses from (**A**) a normal-hearing cat, (**B**) a congenitally deaf cat that was untreated, and (**C**) a congenitally deaf cat that received 3 months of electrical stimulation from a cochlear implant. All micrographs were collected from cats that were 6 months of age. The hearing and treated cats exhibit synapses that are punctate, curved, and accompanied by nearby synaptic vesicles (asterisks). In contrast, the synapses from untreated deaf cats are large, flattened, and mostly void of synaptic vesicles (arrowheads). Scale bar, 0.5 μm.
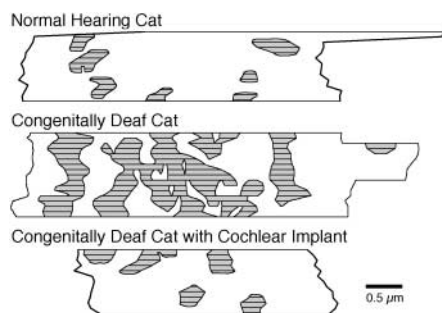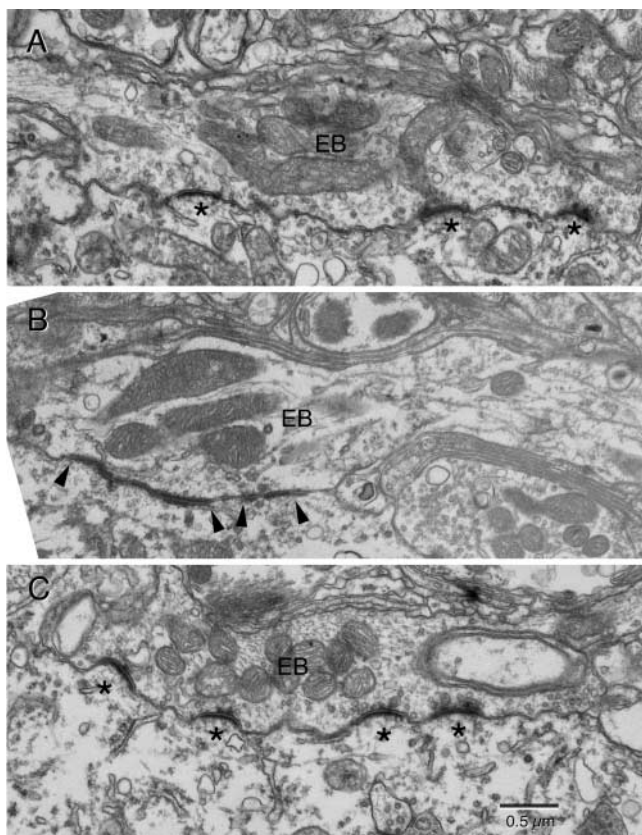
Fig. 3. Postsynaptic densities from endbulbs of Held, indicative of release sites, were reconstructed through serial sections using three-dimensional software and then rotated. These views present the surface of the bushy cell membrane that lies under the auditory nerve ending. The shaded and lined regions represent the reconstructed synapses. Each horizontal line indicates a single ultrathin section. The congenitally deaf cats exhibited hypertrophied synapses, whereas the stimulated deaf cats exhibited synapses having normal shapes and distributions.

membrane (Fig. 3). The reconstructed area of individual postsynaptic densities from normal-hearing cats averaged 0.127 ± 0.071 μm² ($n = 129$). In contrast, the endbulb synapses of congenitally deaf cats exhibited distinct differences. There was a reduction in the number of synaptic vesicles, and the postsynaptic densities appeared flattened, thicker, and longer (Fig. 2). When individual postsynaptic densities were reconstructed through serial sections, they

were hypertrophied (Fig. 3), averaging 0.301 ± 0.398 μm² ($n = 152$).

In stimulated deaf cats, endbulb synapses resembled those from normal-hearing cats (Fig. 2). The full complement of synaptic vesicles was present, and the curvature of the typical normal postsynaptic density had returned. When the postsynaptic densities from the implanted cats were reconstructed through serial sections, they were normal in size (0.093 ± 0.078 μm², $n = 58$) and spatial distribution (Fig. 3). Analysis of variance revealed that there was no significant difference between the size of postsynaptic densities from the auditory nerve fibers of normal-hearing and implanted cats, whereas those from congenitally deaf cats were significantly larger ($P < 0.001$). If these cats had not received such treatment, their synapses would have remained pathologic (2).

The importance of neural activity for normal development and function of sensory systems is well documented (23–27). There is growing evidence to suggest that prosthetic stimulation serves as an adequate substitution. Induced neural activity by electrical stimulation in deaf cats has been reported to restore cell size in the region of the cochlear nucleus innervated by endbulbs (28–30), an effect presumably mediated by the restored synapses. Without stimulation, the cells were shrunken (31, 32). These data establish that the morphology of central auditory synapses is malleable not only to deprivation but also to stimulation.

The functional importance of synaptic recovery in auditory nerve fibers is that temporal processing is improved in the chronically stimulated cats. Preservation of the "timing pathway" through the endbulb–bushy cell circuit would support the precise transmission of temporal cues within the auditory signal. Because the cochlear nucleus gives rise to all ascending auditory pathways, the normalization of synapses is hypothesized to enable the faithful transmission of auditory signals throughout the system. Temporal resolution of neurons in the inferior colliculus demonstrated impaired frequency following of neurons in neonatally deafened cats. This impaired frequency following improved after electrical stimulation of the cochlea (16). The critical nature of temporal resolution in facilitating speech recognition is underscored by studies that show speech recognition based on temporal cues while spectral content is systematically degraded (33). From the cochlear nucleus, high-fidelity temporal features of sound can be used to mediate more complex functions occurring in auditory cortex (15, 34, 35). It is logical to infer that deafness results in synaptic abnormalities in auditory nerve fibers of congenitally deaf humans, similar to those found in other mammals. We hypothesize that the changes observed after cochlear implantation at this crucial synapse enable the development of integrative and cognitive brain functions reflected in aural and oral communication in deaf children (1, 17–19, 36, 37).

References and Notes
1. H. W. Francis, J. K. Niparko, *Pediatr. Clin. North Am.* **50**, 341 (2003).
2. D. K. Ryugo, T. Pongstaporn, D. M. Huchton, J. K. Niparko, *J. Comp. Neurol.* **385**, 230 (1997).
3. D. K. Ryugo, B. T. Rosenbaum, P. J. Kim, J. K. Niparko, A. A. Saada, *J. Comp. Neurol.* **397**, 532 (1998).
4. D. J. Lee, H. B. Cahill, D. K. Ryugo, *J. Neurocytol.* **32**, 229 (2003).
5. D. K. Ryugo, D. M. Fekete, *J. Comp. Neurol.* **210**, 239 (1982).
6. R. R. Pfeiffer, *Science* **154**, 667 (1966).
7. A. L. Babalian, D. K. Ryugo, E. M. Rouiller, *Exp. Brain Res.* **153**, 452 (2003).
8. C. E. Carr, *Annu. Rev. Neurosci.* **16**, 223 (1993).
9. L. O. Trussell, *Curr. Opin. Neurobiol.* **12**, 400 (2002).
10. C. J. Limb, D. K. Ryugo, *J. Assoc. Res. Otolaryngol.* **1**, 103 (2000).
11. S. Oleskevich, B. Walmsley, *J. Physiol.* **540**, 447 (2002).
12. S. Oleskevich, M. Youssoufian, B. Walmsley, *J. Physiol.* **560**, 709 (2004).
13. R. K. Shepherd, J. H. Baxi, N. A. Hardie, *J. Neurophysiol.* **82**, 1363 (1999).
14. A. Kral, J. Tillein, S. Heid, R. Hartmann, R. Klinke, *Cereb. Cortex* **15**, 552 (2005).
15. R. Klinke, A. Kral, S. Heid, J. Tillein, R. Hartmann, *Science* **285**, 1729 (1999).
16. M. Vollmer, P. A. Leake, R. E. Beitel, S. J. Rebscher, R. L. Snyder, *J. Neurophysiol.* **93**, 3339 (2005).
17. A. K. Cheng, J. K. Niparko, *Arch. Otolaryngol. Head Neck Surg.* **125**, 1214 (1999).
18. P. A. Busby, G. M. Clark, *J. Acoust. Soc. Am.* **105**, 1841 (1999).
19. R. Taitelbaum-Swead et al., *Int. J. Pediatr. Otorhinolaryngol.*, in press.
20. J. H. Frijns, J. J. Briaire, J. A. de Laat, J. J. Grote, *Ear Hear.* **23**, 184 (2002).
21. N. J. Lenn, T. S. Reese, *Am. J. Anat.* **118**, 375 (1966).
22. N. B. Cant, D. K. Morest, *Neurosci.* **4**, 1925 (1979).
23. T. N. Wiesel, D. H. Hubel, *J. Neurophysiol.* **26**, 973 (1963).

24. H. Van der Loos, T. A. Woolsey, *Science* **179**, 395 (1973).
25. E. Meisami, *Prog. Brain Res.* **48**, 211 (1978).
26. E. W. Rubel, B. Fritzsch, *Annu. Rev. Neurosci.* **25**, 51 (2002).
27. L. C. Katz, C. J. Shatz, *Science* **274**, 1133 (1996).
28. J.-I. Matsushima, R. K. Shepherd, H. L. Seldon, S.-A. Xu, G. M. Clark, *Hear. Res.* **56**, 133 (1991).
29. L. R. Lustig, P. A. Leake, R. L. Snyder, S. J. Rebscher, *Hear. Res.* **74**, 29 (1994).
30. A. Kawano, E. Hakuhisa, S. Funasaka, *Nip. Jibiin. Gak. Kaiho* **99**, 884 (1996).
31. C. D. West, J. M. Harrison, *J. Comp. Neurol.* **151**, 377 (1973).
32. A. A. Saada, J. K. Niparko, D. K. Ryugo, *Brain Res.* **736**, 315 (1996).
33. R. V. Shannon, F. G. Zeng, V. Kamath, J. Wygonski, M. Ekelid, *Science* **270**, 303 (1995).
34. Y. Naito et al., *Acta Otolaryngol.* **117**, 490 (1997).
35. A. Kral, R. Hartmann, J. Tillein, S. Heid, R. Klinke, *Cereb. Cortex* **12**, 797 (2002).
36. A. McConkey Robbins, D. B. Koch, M. J. Osberger, S. Zimmerman-Phillips, L. Kishon-Rabin, *Arch. Otolaryngol. Head Neck Surg.* **130**, 570 (2004).
37. M. A. Svirsky, S. W. Teoh, H. Neuburger, *Audiol. Neurootol.* **9**, 224 (2004).
38. The authors thank C. A. Haenggeli and C. Limb for helping with the surgeries, T. Pongstaphone for electron microscopic assistance, K. Montey for histological assistance, and M. Muniak for video editing. This work was supported by NIH grants RO1 DC00232 and F31 DC05864, The Emma Liepmann Endowment Fund, and a grant from the Advanced Bionics Corporation (Sylmar, CA).

A Role for the Phagosome in Cytokine Secretion

Rachael Z. Murray, Jason G. Kay, Daniele G. Sangermani, Jennifer L. Stow*

Membrane traffic in activated macrophages is required for two critical events in innate immunity: proinflammatory cytokine secretion and phagocytosis of pathogens. We found a joint trafficking pathway linking both actions, which may economize membrane transport and augment the immune response. Tumor necrosis factor α (TNFα) is trafficked from the Golgi to the recycling endosome (RE), where vesicle-associated membrane protein 3 mediates its delivery to the cell surface at the site of phagocytic cup formation. Fusion of the RE at the cup simultaneously allows rapid release of TNFα and expands the membrane for phagocytosis.

In response to a microbial challenge, activated macrophages initiate multiple actions, including the secretion of proinflammatory cytokines and the phagocytosis of microorganisms (*1*).

Both of these actions require substantial up-regulation of protein trafficking and deployment of membrane to the cell surface. TNFα, the earliest and most potent proinflammatory cytokine released, has an essential role in immunity but also plays a causative role in inflammatory disease (*2*). The secretory pathway for the trafficking of the newly synthesized transmembrane form of TNFα to the cell surface is unknown. Our approach has been to identify specific vesicular machinery that functions in this pathway (*3*, *4*). Soluble N-ethylmaleimide–sensitive factor (NSF) attachment receptor (SNARE)–mediated fusion of vesicular carriers is a requirement of this and other trafficking pathways (*5*). Q-SNARE complexes on the Golgi (syntaxin 6–syntaxin 7–Vti1b) and at the cell surface [syntaxin 4–SNAP23 (synaptosomal-associated protein of 23 kD)] function in and are rate-limiting for TNFα trafficking and secretion (*3*, *4*). A microarray

Institute for Molecular Bioscience, University of Queensland, Brisbane, Queensland 4072, Australia.

*To whom correspondence should be addressed. E-mail: j.stow@imb.uq.edu.au

Fig. 1. VAMP3 up-regulation and function as the R-SNARE for TNFα secretion. (**A**) VAMP3 protein expression: up-regulation by LPS compared with other relevant SNAREs and in IFN-primed cells. WB, Western blotting. (**B**) SNARE partners coimmunoprecipitated (IP) with VAMP3 or VAMP8 are detected by immunoblotting. (**C**) TNFα secreted into media of transfected cells (GFP alone or GFP-VAMP3) measured by enzyme-linked immunosorbent assay (ELISA). Error bar indicates SEM. (**D**) Surface TNFα stained on unpermeabilized, TACE inhibitor–treated cells. Bar graph shows proportion of cells expressing GFP alone or GFP-VAMP3(1–81) mutant with >2-fold reduction in surface TNFα-staining expression. (**E**) Targeted knockdown of VAMP3 protein using three different specific siRNAs (left), and surface staining of TNFα in control (no siRNA) or siRNA-transfected cells (right) (*23*).